Published in final edited form as:
Curr Biol. 2008 July 22; 18(14): 1055–1061. doi:10.1016/j.cub.2008.06.046.

Changes in *bicoid* mRNA anchoring highlight conserved mechanisms during the oocyte-to-embryo transition

Timothy T. Weil[1], **Richard Parton**[2,3], **Ilan Davis**[2,3], and **Elizabeth R. Gavis**[1*]

1*Department of Molecular Biology, Princeton University, Princeton, NJ 08544, USA*

2*Department of Biochemistry, The University of Oxford, South Parks Road, Oxford OX1 3QU, UK*

Summary

Intracellular mRNA localization directs protein synthesis to particular subcellular domains to establish embryonic polarity in a wide range of vertebrates and invertebrates. In *Drosophila*, *bicoid* (*bcd*) mRNA is pre-localized at the anterior of the oocyte. After fertilization, this RNA is translated to produce a Bcd protein gradient that determines anterior cell fates [1,2]. Recent analysis of *bcd* mRNA during late stages of oogenesis led to a model for steady-state localization of *bcd* by continual active transport [3]. Here, we elucidate the path and mechanism of sustained *bcd* mRNA transport by direct observation of *bcd* RNA particle translocation in living oocytes. However, this mechanism cannot explain maintenance of *bcd* localization throughout the end of oogenesis, when microtubules disassemble in preparation for embryogenesis [4,5] or retention of *bcd* at the anterior in mature oocytes, which can remain dormant, but developmentally competent, for weeks prior to fertilization [6]. Through temporal analysis of *bcd* RNA particle dynamics, we show that *bcd* mRNA shifts from continuous active transport to stable actin-dependent anchoring at the end of oogenesis, ensuring the developmental integrity of the oocyte during dormancy. Egg activation triggers release of *bcd* from the anterior cortex for proper deployment in the fertilized egg, probably through reorganization of the actin cytoskeleton. These findings uncover a surprising parallel between flies and frogs, as cortically tethered *Xenopus Vg1*mRNA undergoes a similar redistribution during oocyte maturation [7]. Our results highlight a conserved mechanism used by invertebrates and vertebrates to regulate mRNA anchoring and redeployment during the oocyte-to-embryo transition.

Results and Discussion

Using live cell imaging of mRNA labeled in vivo with GFP or RFP, we previously determined that *bcd* mRNA accumulates at the anterior cortex primarily late in oogenesis, as the ovarian nurse cells extrude their cytoplasm into the oocyte, a process known as nurse cell dumping [3]. This localization requires a special population of microtubules that are anchored to the anterior cortical actin cytoskeleton. Concurrently, *nanos* (*nos*) mRNA accumulates at the oocyte posterior, but unlike *bcd*, *nos* localization is microtubule-independent [8]. Fluorescence recovery after photobleaching (FRAP) analysis showed that, at steady state, the population of *bcd* mRNA at the anterior cortex remains in flux. In contrast, the population of *nanos* (*nos*) mRNA localized at the posterior pole of the oocyte is static [3]. To elucidate the mechanistic

*Author for correspondence: lgavis@princeton.edu; Phone: (609) 258-3857; FAX: (609) 258-1343.
[3]Former address: Wellcome Trust Centre for Cell Biology, The University of Edinburgh, The Kings Buildings, Edinburgh EH9 3JR, UK

basis for this difference between *bcd* and *nos*, we visualized RNA particles in oocytes expressing GFP-labeled *bcd* or *nos* mRNA (*bcd*GFP* or *nos*GFP*) [3,8] using widefield imaging methods that allow increased sensitivity and temporal resolution.

Drosophila oogenesis progresses through 14 morphologically defined stages. Dumping, which transfers *bcd* and *nos* to the oocyte, initiates at stage 10b, and is accompanied by vigorous movement of the oocyte cytoplasm (ooplasmic streaming) that mixes the oocyte and incoming nurse cell cytoplasm. Particles of *bcd*GFP* are highly dynamic during stages 10b-13, even after dumping and ooplasmic streaming have ceased (Figure 1A, 1B, 1Ba–Bf, 1E, 1F; Movie S1; data not shown). In contrast, little movement was detected among *nos*GFP* particles visualized at the oocyte posterior (Fig 1C, D; Movie S1).

To establish whether *bcd* mRNA particles move in a directed manner, we monitored all particles within representative regions of the anterior or posterior oocyte cortex. Particles were scored as static (no significant detectable movement), jiggling (movement within one particle length in any direction), or directed (sustained runs of more than 1 μm in a single direction) (Fig 1E, F). Among 11 stage 10b-13 oocytes, we observed movement by 85% (n = 283/332) of *bcd*GFP* particles (Table 1). Nearly 25% of these show directed runs, but this value is likely an underestimate since we were unable to track particles that moved rapidly in or out of the plane of focus. While the majority of particles were detected within 5 μm of the cortex, *bcd*GFP* particles undergoing directed movement could be detected as far as 20 μm from the anterior.

Tracking of individual particles showed that 70% travel toward or laterally along the anterior cortex and 30% travel away from the anterior, with average instantaneous velocities of 0.36–2.15 μm/sec (Fig 1E, F). Occasionally, *bcd*GFP* particles exhibit pauses during runs and, more rarely, direction reversals (Movie S2, S3). In addition, complex trajectories were observed that suggest translocation of particles between microtubules (Movie S4). In contrast to *bcd*, only 12% (n = 21/174) of *nos*GFP* particles at the posterior cortex exhibit any detectable movement and all of this movement is due to jiggling (Table 1). We also detected flow of *nos*GFP* particles in concert with yolk granules during ooplasmic streaming, consistent with passive movement (Fig 1D; Movie S1).

The directed runs of *bcd* particles we observed suggest translocation on microtubules. We tested this hypothesis by covisualizing microtubules labeled with tau-GFP together with *bcd*GFP* in stage 12 oocytes. Our results show individual *bcd*GFP* particles moving along microtubule tracks, providing direct in vivo evidence for microtubule-based RNA transport (Figure 2A–2C; Movie S5). Previous work is consistent with transport of *bcd* mRNA in late oocytes being Dynein-dependent [3]. To test this hypothesis directly, we analyzed the effect of hypomorphic mutations in Dynein heavy chain (*Dhc*), the force generating motor subunit, on *bcd* particle movement. We found that all movement of *bcd*GFP particles is completely eliminated in *Dhc* mutant oocytes, including both unidirectional and bidirectional motility (Movie S6). These observations are consistent with recent evidence that Dynein can mediate both minus- and plus-end directed transport [9–11]. The minimal amount of *bcd* detected at the anterior cortex could be due to residual Dynein function of the hypomorphic alleles used, which is sufficient at least to permit oogenesis (Figure 2D–2F). Alternatively, this RNA may have been localized during mid-oogenesis, when anchoring is microtubule-independent [3], a notion that is supported by the fact that in contrast to *bcd*GFP* particles at the anterior of wild-type oocytes, residual *bcd*GFP* particles in *Dhc* mutant oocytes are stationary. Taken together, these results provide direct visual evidence that *bcd* is transported to the anterior on microtubules by dynein, and that sustained transport achieves steady-state anterior localization.

Following dumping, oogenesis proceeds very rapidly to produce a mature oocyte in approximately 8 hours. In contrast, mature (stage 14) oocytes are long lived and can be stored for weeks by the female prior to fertilization. These stored oocytes appear to be physiologically stable as they give rise to viable progeny[6]. It remained unclear whether *bcd* mRNA transport is sustained during stage 14 for long periods by continuous active transport or, alternatively, whether *bcd* mRNA transitions to a stably anchored state to ensure maintenance over long time periods. We distinguished between these two possibilities by analyzing the dynamics of *bcd* RNA particles at successive stages of oogenesis after the onset of dumping. We found a marked decrease in the frequency of directed runs as oogenesis progresses in laying females (Table 1). By stage 14, all mobility declines as particles coalesce to form large, stationary foci at the anterior cortex (Figure 3A–3E,Movie S7). These foci remain associated with the anterior cortex through stage 14 and appear to be composed of many individual *bcd* particles (Figure 3F;Movie S8). Consistent with their ability to support normal development, *bcd* remains localized in stage 14 oocytes held for several days by unfertilized females (data not shown).*bcd* RNA particles contain Staufen (Stau), a double-stranded RNA binding protein required for *bcd* localization from stage 10b onward [3,12], and this association is maintained when particles coalesce into foci (Figure 3F–3H).*nos* particles, which are anchored to the actin cytoskeleton, do not change their distribution at the posterior cortex during this time (data not shown). These results are consistent with the acquisition of a stable cortical anchoring mechanism for *bcd* toward the end of oogenesis.

Maintenance of *bcd* at the anterior cortex during stages 10b-13 is both microtubule and actin-dependent. The actin-dependence at these stages is indirect, however, through a requirement for actin in anchoring microtubules to the anterior cortex [3]. To test the role of the cytoskeleton in stable *bcd* mRNA anchoring at stage 14, we studied the effects of actin and microtubule depolymerizing drugs on *bcd* mRNA localization at the final stage of oogenesis. Treatment of stage 14 oocytes with the microtubule depolymerizing drug colcemid, either in culture or through ingestion by females, did not affect maintenance of *bcd*GFP* foci at the anterior (data not shown). In contrast, treatment of cultured stage 14 oocytes with cytochalasin D (cyto D) to disrupt the actin cytoskeleton resulted in dissociation of *bcd*GFP* foci from the anterior and their dispersion into individual particles (Figure 3I, 3J). We conclude that maintenance of *bcd* by continual transport is replaced by an actin-based anchoring mechanism by the end of oogenesis, ensuring the developmental integrity of the mature oocyte.

Embryogenesis marks a new phase, in which pre-localized *bcd* mRNA is translated for the first time to produce the morphogenetic Bcd gradient. Since Bcd protein concentration is linearly related to the amount of *bcd* mRNA [13], cortically anchored *bcd* foci could provide concentrated point sources in the fertilized embryo to generate the peak Bcd concentration. However, through visualization of *bcd*GFP*, we found that *bcd* undergoes a final transition from its localization in cortical foci at stage 14, becoming dispersed as fine particles throughout the anterior region of the newly fertilized embryo (Figure 4A–4C). These particles retain Stau, suggesting that the RNA particle composition is not grossly altered during this reorganization (Figure 3K–3M). Time lapse imaging showed that *bcd*GFP particles do not exhibit directed movement in the embryo but remain fixed in place as though tethered (data not shown).

The transition from oogenesis to embryogenesis requires calcium dependent events, collectively termed "egg activation", that occur inside the female to allow the newly fertilized egg to complete meiosis and initiate embryonic development [14–17]. We tested whether egg activation triggers the redistribution of *bcd* RNA, using stage 14 oocytes activated in vitro. We found that egg activation eliminates or severely reduces foci of *bcd*GFP*; instead, *bcd*GFP* particles become dispersed within the anterior region, resembling their distribution in the embryo (Figure 4D–4F). Time lapse imaging showed that foci begin to dissipate within 3–5 minutes of activation (Figure S1A–S1C). The requirement for actin in *bcd* anchoring at stage

14 prompted us to investigate whether egg activation might affect *bcd* localization by regulating the actin cytoskeleton. The actin cytoskeleton was monitored using a GFP fusion to the F-actin binding tail of moesin (GFP-moe), which decorates cortical actin without disrupting actin function [18]. When visualized at stage 14, the actin cytoskeleton appears dense and tightly apposed to the oocyte cortex (Figure 4G, 4Ga, 4Gb). In vitro egg activation causes a rapid alteration in actin organization, producing a diffuse actin network that extends into the interior of the egg (Figure 4H, 4Ha, 4Hb). A similar distribution of actin is observed in the newly fertilized embryo (Figure 4I). Moreover, this rearrangement of the actin cytoskeleton can be detected within 3 minutes of activation, corresponding to the onset of *bcd* dispersal (Figure S1D–S1F).

To confirm that the change in *bcd* localization is indeed a physiological consequence of egg activation, we examined the effect of mutations that disrupt egg activation on *bcd* localization in the early embryo. *sarah*(*sra*) encodes calcipressin, an inhibitor of the calcium dependent phosphatase calcineurin, and acts early in the egg activation pathway [16,17]. In contrast to wild-type embryos, *bcd*GFP* remains cortically associated in *sra* mutant embryos and forms foci characteristic of stage 14 oocytes (Figure 5A–5C). However, mutations in two other genes required during egg activation, *cortex (cort)*, which encodes a Cdc20 family member [5,19] and *grauzone* (*grau*), which activates *cort* expression [20], do not prevent redistribution of *bcd*GFP* (Figure 5D–5F). The timing of *bcd* dispersal and its dependence on *sra*, but not *cort* or *grau*, lead us to conclude that an early, *sarah*-dependent event during egg activation triggers redistribution of *bcd* RNA for embryogenesis. Given Sra's function as a calcium regulator [16,17], we propose that this event is likely to involve calcium signalling.

Together, our studies show that as oogenesis proceeds toward formation of a developmentally competent egg, *bcd* mRNA transitions from being continuously transported to a stably anchored state. By providing a mechanism to ensure *bcd* localization for long periods of time in dormant stage 14 oocytes, stable anchoring may play an important role in buffering reproduction against environmental challenges. The delay in stable anchoring of *bcd* mRNA at the anterior may be caused by the rapid influx of nurse cell cytoplasm occurring at the oocyte anterior during dumping. Alternatively, deployment of this anchoring mechanism may require factors provided to the oocyte during dumping. In either case, continual transport provides a mechanism to retain *bcd* at the anterior until other developmental processes are complete. Previous work has shown that cortically associated microtubules are replaced by short, randomly oriented cytoplasmic microtubules as the oocyte matures during stages 13–14 [4]. These cytoplasmic microtubules disappear by fertilization [5], when microtubules are nucleated by centrosomes for nuclear divisions and migration [21]. Although we have not been able to determine if and when the specific anterior population of microtubules that transport *bcd* is disassembled, it is likely that disassembly of oocyte microtubules in preparation for embryogenesis is coordinated with, or required for *bcd* mRNA anchoring.

A surprising finding is the release of *bcd* from its anterior cortical tether during egg activation. In the early embryo, *bcd* mRNA particles contain Stau, indicating release from the anterior cortex does not result from disassembly of *bcd*/Stau complexes (Figure 3K–M). Rather, our results suggest a mechanism for release of *bcd* from the cortex by an activation-dependent re-structuring of the actin cytoskeleton. Interestingly, a similar mechanism may be used in Xenopus oocytes for the disassociation of localized *Vg1* mRNA from the vegetal cortex. Like *bcd*, release of *Vg1* mRNA is triggered by egg activation and can be mimicked by pharmacological disruption of the actin cytoskeleton [7]. Dispersal of Vg1 mRNA prior to cleavage divisions presumably promotes its inheritance by vegetal cells, where production of Vg1 protein is required for mesoderm induction and embryonic patterning [22]. We propose that, in addition to cell cycle progression, a conserved feature of egg activation is the redeployment of mRNAs localized during oogenesis for their embryonic functions.

Conclusion

Although the molecular determinants of embryonic patterning may differ between invertebrates and vertebrates, mRNA localization plays a fundamental role in the deployment of key patterning molecules in both *Drosophila* and *Xenopus*. It is well recognized that while RNA cargos may not be conserved, the machinery for delivering these cargos to the correct destinations is [23,24]. Our findings suggest that these parallels go even deeper to include mRNA anchoring and redeployment mechanisms that act during the transition from oogenesis to embryogenesis to ensure proper patterning.

Experimental Procedures

Fly strains

The following mutants and transgenic lines were used: $Dhc^{6\text{-}6}$, $Dhc^{6\text{-}12}$(ref [25]); sra^{A108}, sra^{687} (ref [16]); $cort^{QW55}$, $cort^{RH65}$, $grau^{QQ36}$, $grau^{RG1}$ (refs [5,26]); *hsp83-MCP-GFP*, *hsp83-MCP-RFP*, $bcd\text{-}(ms2)_6$(ref [3]); $nos\text{-}(ms2)_{18}$(ref [27]), *tau-GFP*(ref [28]); *GFP-Stau* (ref [29]); *GFP-moe* (sGMCA; ref [18]). The $bcd\text{-}(ms2)_6$ and $nos\text{-}(ms2)_{18}$ transgenes completely rescue the *bcd* and *nos* mutant patterning defects, respectively [3,27].

Manipulation and confocal imaging of oocytes and embryos

Oocytes were cultured and treated with cytochalasin D (Sigma; 10 μg/ml final concentration) or colcemid (Sigma; final concentration 50 μg/ml) as previously described [3]. For colcemid feeding, fresh females were starved for 2–3 days, then for 4 hours with fed yeast paste supplemented to 50 μg/ml colcemid. In vitro activation of stage 14 oocytes was carried out according to Page and Orr-Weaver [30] with modification: individual stage 14 oocytes from well fed females were dissected in Schneider's insect culture medium (GIBCO-BRL) and individual egg chambers were transferred to uncoated #1.5 glass bottom culture dishes (MatTek) and covered with a 1 mm^2 coverslip cut from a #1.5 glass coverslip (Corning). Schneider's medium was then removed and replaced by activation buffer [30]. Embryos were collected for 0–2 hour periods on yeasted apple juice agar plates, dechorionated for 1 minute in 50% bleach, then mounted on No. 1 coverslips and covered with Series 95 halocarbon oil. Time-lapse and Z-series imaging were carried out using a Leica TCS SP5 confocal microscope, 63x/1.3 NA objective.

For co-visualization of *bcd* and Stau, ovaries expressing *bcd*RFP* and GFP-Stau were dissected into Schneider's medium and isolated egg chambers were imaged directly. Embryos from females expressing *bcd*GFP* were fixed in 1:5 4% paraformaldehyde/PBS:heptane for 20 minutes, washed with PBS, and vitelline membranes were removed manually. Anti-Stau immunostaining was performed using 1:2000 rabbit anti-Stau (gift of D. St Johnston) and 1:1000 Alexa Fluor 568 goat anti-rabbit (Invitrogen/Molecular Probes). Embryos were mounted in Aqua PolyMount (Polysciences, Inc) and imaged with a Zeiss LSM510 confocal microscope.

Live imaging and analysis of RNA particles

Ovaries from well fed females were dissected in Series 95 halocarbon oil (KMZ Chemicals) onto No. 1 coverslips (Corning) and separated from ovarioles using tungsten needles. Time lapse imaging was performed using a wide-field DeltaVision microscope (Applied Precision, Olympus IX70 microscope, Coolsnap HQ [Roper] camera) with 100x/1.35NA objective. Images were deconvolved using Sedat/Agard algorithms with Applied Precision software [31]. Particle movement was analyzed and tracked semi-manually, using Image-Pro Plus (Leeds) and Metamorph (Universal Imaging Corporation) software packages.

Supplementary Material

Refer to Web version on PubMed Central for supplementary material.

Acknowledgements

We thank T. Hays, D. Kiehart, A. Martin, T. Schüpbach, M. Welte, and M. Wolfner for fly stocks, D. St Johnston for fly stocks and anti-Stau antibody, J. Goodhouse for assistance with confocal microscopy, and T. Schüpbach and E. Wieschaus for comments on the manuscript. This work was supported by a grant from the National Institutes of Health (GM067758) to E.R.G. and Senior Fellowship from the Wellcome Trust to I.D.

References

1. Driever W, Nüsslein-Volhard C. The *bicoid* protein determines position in the *Drosophila* embryo in a concentration-dependent manner. Cell 1988;54:95–104. [PubMed: 3383245]
2. Berleth T, Burri M, Thoma G, Bopp D, Richstein S, Frigerio G, Noll M, Nüsslein-Volhard C. The role of localization of *bicoid* RNA in organizing the anterior pattern of the *Drosophila* embryo. EMBO J 1988;7:1749–1756. [PubMed: 2901954]
3. Weil TT, Forrest KM, Gavis ER. Localization of *bicoid* mRNA in late oocytes is maintained by continual active transport. Dev. Cell 2006;11:251–262. [PubMed: 16890164]
4. Theurkauf WE, Smiley S, Wong ML, Alberts BM. Reorganization of the cytoskeleton during *Drosophila* oogenesis: implications for axis specification and intercellular transport. Development 1992;115:923–936. [PubMed: 1451668]
5. Page AW, Orr-Weaver TL. The *Drosophila* genes *grauzone* and *cortex* are necessary for proper female meiosis. J. Cell Sci 1996;109:1707–1715. [PubMed: 8832393]
6. Wyman R. The temporal stability of the *Drosophila* oocyte. J. Embryol. Exp. Morphol 1979;50:137–144. [PubMed: 110902]
7. Yisraeli JK, Sokol S, Melton DA. A two-step model for the localization of maternal mRNA in *Xenopus* oocytes: Involvement of microtubules and microfilaments in the translocation and anchoring of Vg1 mRNA. Development 1990;108:289–298. [PubMed: 2351071]
8. Forrest KM, Gavis ER. Live imaging of endogenous mRNA reveals a diffusion and entrapment mechanism for *nanos* mRNA localization in *Drosophila*. Curr. Biol 2003;13:1159–1168. [PubMed: 12867026]
9. Ross JL, Wallace K, Shuman H, Goldman YE, Holzbaur EL. Processive bidirectional motion of dynein-dynactin complexes in vitro. Nat. Cell Biol 2006;8:562–570. [PubMed: 16715075]
10. Gennerich A, Carter AP, Reck-Peterson SL, Vale RD. Force-induced bidirectional stepping of cytoplasmic dynein. Cell 2007;131:952–965. [PubMed: 18045537]
11. Vendra G, Hamilton RS, Davis I. Dynactin suppresses the retrograde movement of apically localized mRNA in *Drosophila* blastoderm embryos. RNA 2007;13:1860–1867. [PubMed: 17901156]
12. St Johnston D, Driever W, Berleth T, Richstein S, Nüsslein-Volhard C. Multiple steps in the localization of *bicoid* RNA to the anterior pole of the *Drosophila* oocyte. Development Suppl 1989;107:13–19.
13. Gregor T, Tank DW, Wieschaus EF, Bialek W. Probing the limits to positional information. Cell 2007;130:153–164. [PubMed: 17632062]
14. Mahowald AP, Goralski TJ, Caulton JH. In vitro activation of *Drosophila* eggs. Dev. Biol 1983;98:437–445. [PubMed: 6409691]
15. Heifetz Y, Yu J, Wolfner MF. Ovulation triggers activation of *Drosophila* oocytes. Dev. Biol 2001;234:416–424. [PubMed: 11397010]
16. Horner VL, Czank A, Jang JK, Singh N, Williams BC, Puro J, Kubli E, Hanes SD, McKim KS, Wolfner MF, et al. The *Drosophila* calcipressin Sarah is required for several aspects of egg activation. Curr. Biol 2006;16:1441–1446. [PubMed: 16860744]
17. Takeo S, Tsuda M, Akahori S, Matsuo T, Aigaki T. The calcineurin regulator Sra plays an essential role in female meiosis in *Drosophila*. Curr. Biol 2006;16:1435–1440. [PubMed: 16860743]

18. Kiehart DP, Galbraith CG, Edwards KA, Rickoll WL, Montague RA. Multiple forces contribute to cell sheet morphogenesis for dorsal closure in *Drosophila*. J. Cell Biol 2000;149:471–490. [PubMed: 10769037]
19. Chu T, Henrion G, Haegeli V, Strickland S. *Cortex*, a *Drosophila* gene required to complete oocyte meiosis, is a member of the Cdc20/fizzy protein family. Genesis 2001;29:141–152. [PubMed: 11252055]
20. Harms E, Chu T, Henrion G, Strickland S. The only function of Grauzone required for *Drosophila* oocyte meiosis is transcriptional activation of the *cortex* gene. Genetics 2000;155:1831–1839. [PubMed: 10924478]
21. Sullivan W, Theurkauf WE. The cytoskeleton and morphogenesis of the early *Drosophila* embryo. Curr. Opin. Cell Biol 1995;7:18–22. [PubMed: 7755985]
22. Birsoy B, Kofron M, Schaible K, Wylie C, Heasman J. Vg 1 is an essential signaling molecule in *Xenopus* development. Development 2006;133:15–20. [PubMed: 16308332]
23. Oleynikov Y, Singer RH. RNA localization: different zipcodes, same postman? Trends Cell. Biol 1998;8:381–383. [PubMed: 9789325]
24. Gavis, ER.; Singer, RH.; Hüttelmaier, S. Localized translation through messenger RNA localization. In: Hershey, JWB.; Mathews, MB.; Sonenberg, N., editors. Translational Control. Cold Spring Harbor, NY: Cold Spring Harbor Laborator Press; 2007. p. 687-717.
25. Gepner J, Li M, Ludmann S, Kortas C, Boylan K, Iyadurai SJ, McGrail M, Hays TS. Cytoplasmic dynein function is essential in *Drosophila melanogaster*. Genetics 1996;142:865–878. [PubMed: 8849893]
26. Schüpbach T, Wieschaus E. Female sterile mutations on the second chromosome of *Drosophila melanogaster*. I. Maternal effect mutations. Genetics 1989;121:101–117. [PubMed: 2492966]
27. Brechbiel JL, Gavis ER. Spatial regulation of *nanos* is required for its function in dendrite morphogenesis. Curr. Biol 2008;18:745–750. [PubMed: 18472422]
28. Micklem DR, Dasgupta R, Elliot H, Gergely F, Davidson C, Brand A, González-Reyes A, St Johnston D. The *mago nashi* gene is required for the polarisation of the oocyte and the formation of perpendicular axes in *Drosophila*. Curr. Biol 1997;7:468–478. [PubMed: 9210377]
29. Schuldt AJ, Adams JH, Davidson CM, Micklem DR, Haseloff J, St Johnston D, Brand AH. Miranda mediates asymmetric protein and RNA localization in the developing nervous system. Genes Dev 1998;12:1847–1857. [PubMed: 9637686]
30. Page AW, Orr-Weaver TL. Activation of the meiotic divisions in *Drosophila* oocytes. Dev. Biol 1997;183:195–207. [PubMed: 9126294]
31. Clark A, Meignin C, Davis I. A Dynein-dependent shortcut rapidly delivers axis determination transcripts into the *Drosophila* oocyte. Development 2007;134:1955–1965. [PubMed: 17442699]

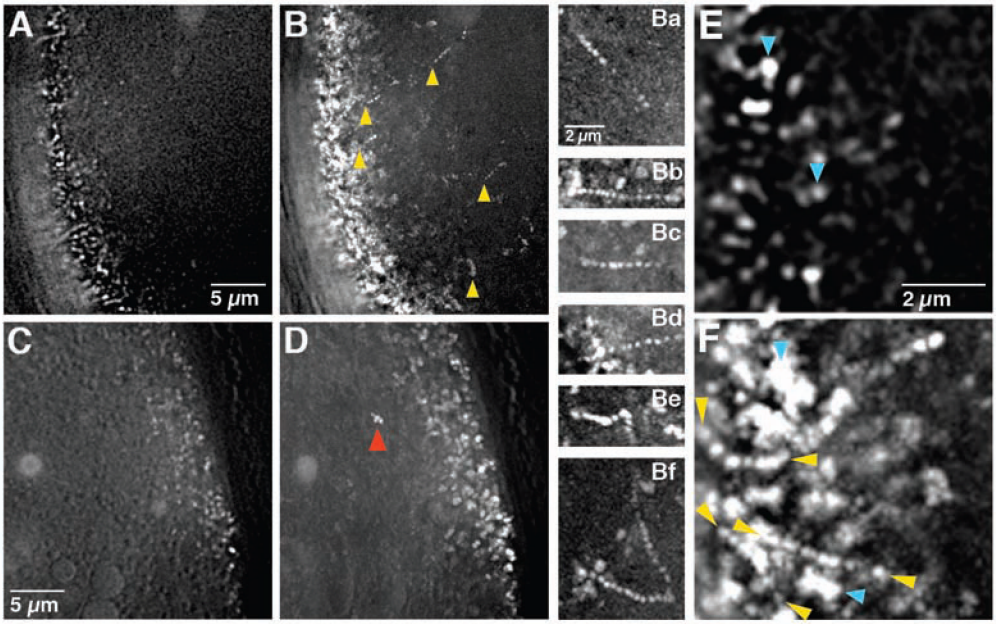

Figure 1. *bcd* and *nos* mRNA particle dynamics in late oocytes

(A–D) Time lapse imaging of *bcd*GFP* (A–B) and *nos*GFP* (C–D) in stage 12 oocytes. (A, C) Starting point (t = 0 sec) of 100 frame time series (Movie S1) taken at the oocyte anterior (A) and posterior (C). (B, D) Trail images in which 100 sequential frames (from t = 0 to t = 29 sec) from the anterior (B) or posterior (D) time series are superimposed. Moving particles appear as sets of dots. Yellow arrowheads in (B) indicate *bcd* RNA particles undergoing directed runs and are positioned at the first point visible in this time sequence. Red arrowhead in (D) indicates a *nos* particle traveling with the ooplasm, which is still streaming in this oocyte. (Ba–Bf) Examples of individual *bcd* RNA particle runs (see Movie S2, Movie S4). (E–F) Higher power time-lapse images of *bcd*GFP* in a stage 12 oocyte. (E) Starting point (t = 0 sec). (F) Trail image compiled from 100 successive frames (from t = 0 to t = 29 sec). Yellow arrowheads indicate directed runs, blue arrowheads indicate jiggling. All images were collected using a DeltaVision microscope and deconvolved (see Experimental Procedures).

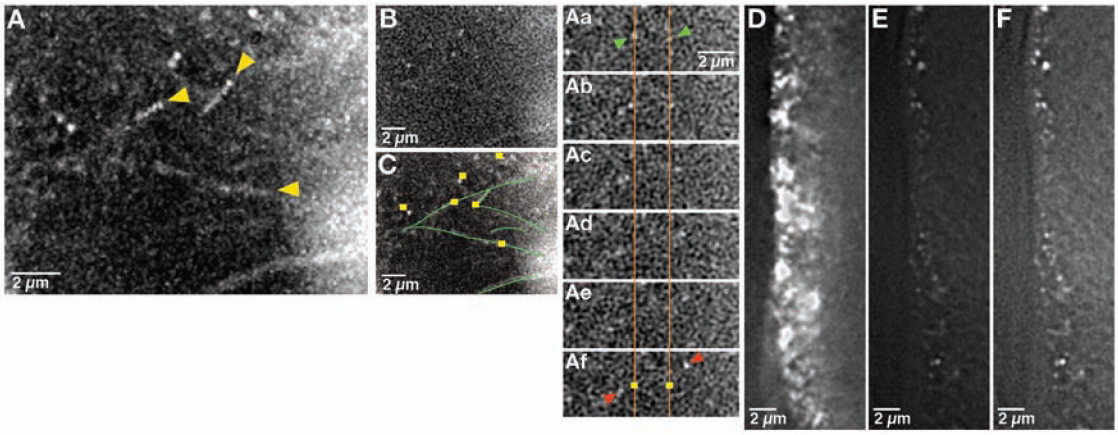

Figure 2. *bcd* RNA particles are transported on microtubules by dynein

(A–C) Region near the anterior cortex of a stage 12 egg oocyte expressing *bcd*GFP* and tau-GFP. Particles can be detected traveling on labeled microtubules at velocities that are indistinguishable from velocities of particles traveling on unlabeled microtubules (see Movie S5). (A) Trail image showing particles traveling on microtubules (yellow arrowheads indicate starting point for each run). (Aa–Af) High power images tracking two representative particles. Orange lines and yellow squares show original starting positions of particles of interest (indicated by green arrowheads in Aa). Red arrows in Af indicate the positions of these particles after 3.5 seconds. (B, C) Single frame at t = 0 for the trail image shown in (A). (C) Schematic based on (A) indicating *bcd* RNA particles (yellow squares) and microtubules (green lines). (D–F) Anterior cortex of a stage 13 oocyte expressing *bcd*GFP* in wild type (D) and $Dhc^{6\text{-}6}$/ $Dhc^{6\text{–}12}$ (E) females. (D) and (E) are displayed at comparable settings, while (F) has been enhanced so that residual *bcd*RNA particles are visible. Particles of *bcd* RNA, visualized using the enhanced setting, show no movement at stage 13 in $Dhc^{6\text{-}6}$/ $Dhc^{6\text{–}12}$ oocytes (see Movie S6). All images were collected using a DeltaVision microscope and deconvolved (see Experimental Procedures).

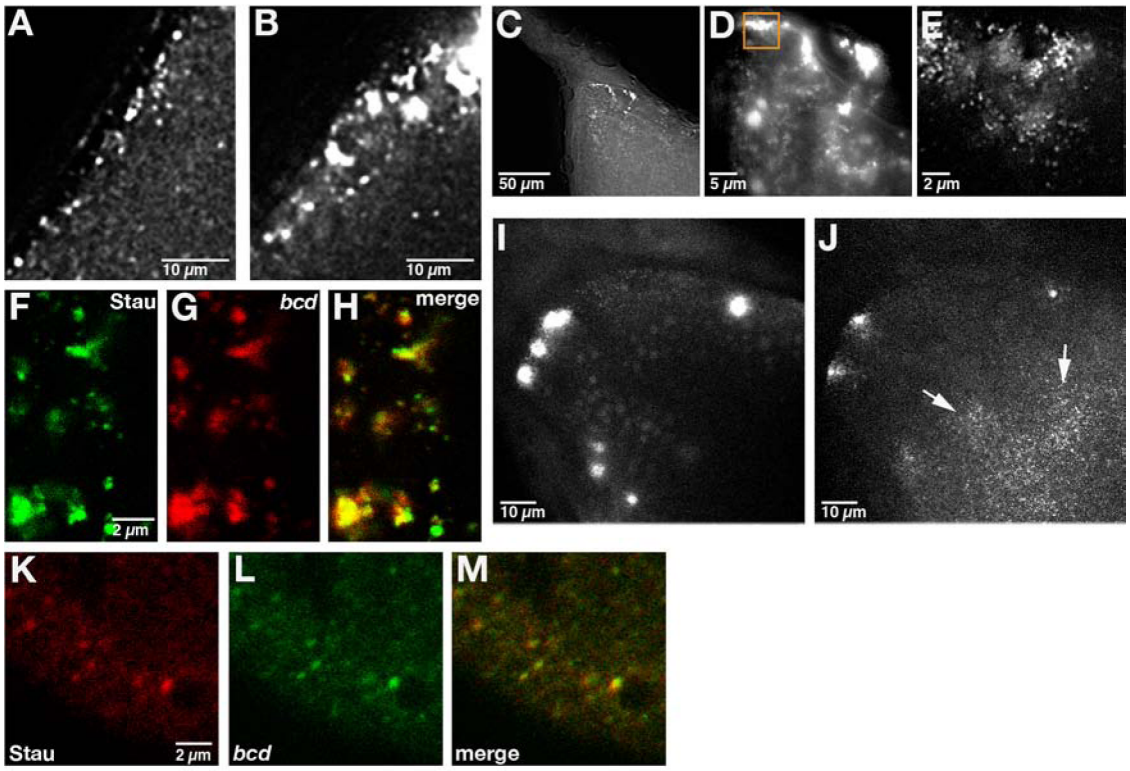

Figure 3. Accumulation and actin-dependent anchoring of *bcd* foci at stage 14

(A, B) Section of a small region at the anterior of (A) stage 13 and (B) stage 14 oocytes expressing *bcd*GFP* (see Movie S7). *bcd* RNA particles coalesce to form large foci at stage 14. (C–E) Section of the anterior of a stage 14 oocyte expressing *bcd*GFP*. (C) 20x magnification; (D) 63x magnification; (E) 100x magnification of region indicated in (D). High magnification shows that these foci are composed of many small particles (see Movie S8). Images in A–E were collected using a DeltaVision microscope and deconvolved (see Experimental Procedures). (F–H) Confocal section of the anterior of a stage 14 oocyte expressing GFP-Stau and *bcd*RFP*. Stau and *bcd* RNA colocalize in large foci at the anterior (H). (I, J) Projections of the anterior of a cultured stage 14 egg chamber expressing *bcd*GFP* imaged (B) prior to and (C) 30 minutes after addition of 10 μg/ml of cytoD to the culture medium. *bcd* RNA foci disperse into small particles (arrows). (K–M) Confocal section of the anterior region of an early embryo expressing *bcd*GFP* and immunostained for Stau. Stau and *bcd* RNA remain colocalized at the anterior in the early embryo as shown in the merged image (K).

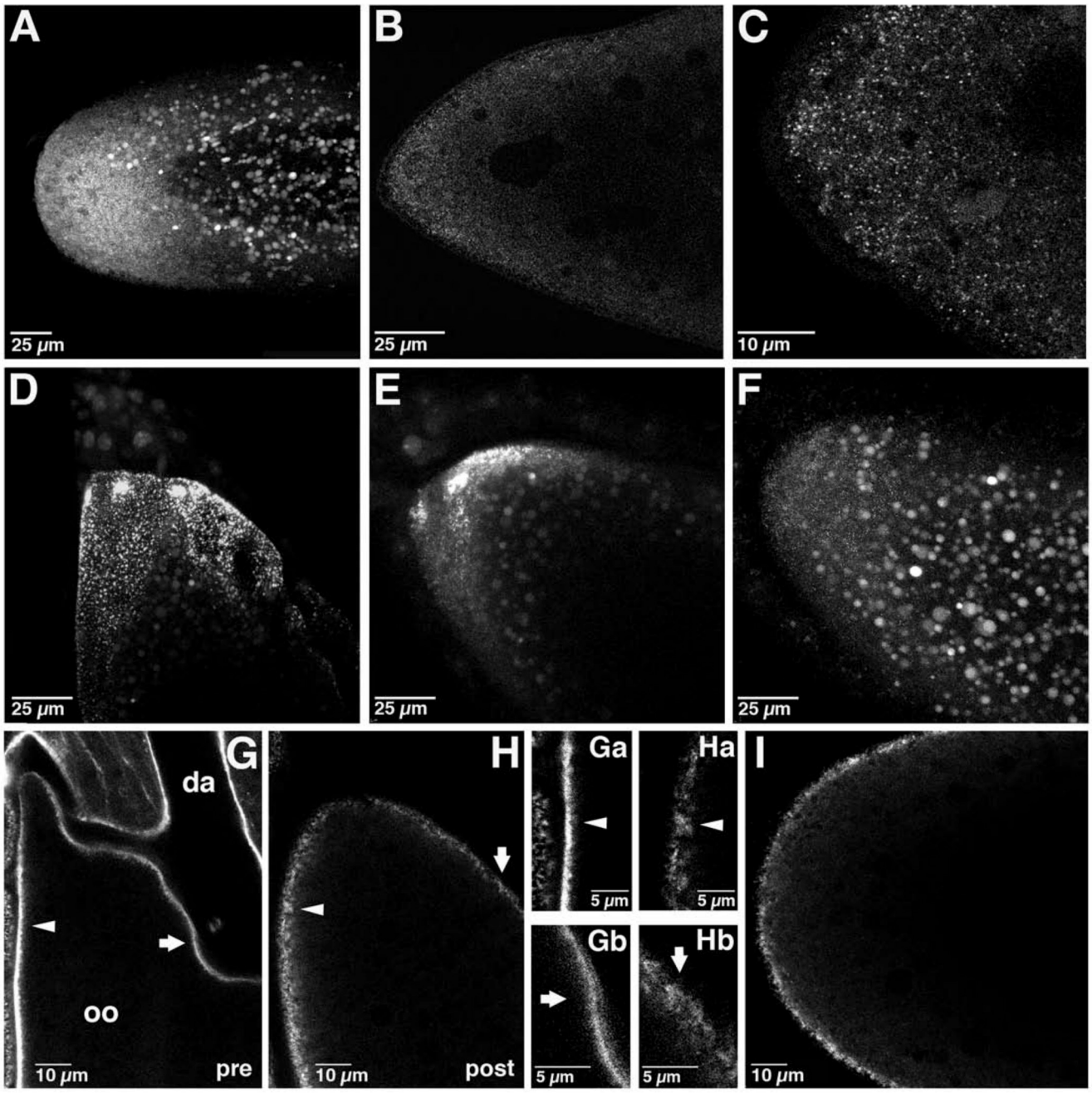

Figure 4. Redistribution of *bcd* and cortical actin during the transition from oogenesis to embryogenesis

(A–C) Anterior region of early embryos expressing *bcd*GFP*. (A) Projection of approximately 52 μm through the anterior half of a newly fertilized embryo. (B) Single confocal section of the anterior region of an early embryo. (C) Confocal section from embryo in (B) taken at higher power. *bcd* mRNA is dispersed in small particles at the anterior in the early embryo. (D–F) In vitro activation of a stage 14 oocyte expressing *bcd*GFP*. Projections of confocal images taken (D) prior to addition of activation buffer, (E) 5 minutes after addition, and (F) 25 minutes after addition. *bcd* mRNA foci disperse into fine particles rapidly upon activation. (G–H) Single confocal sections of oocytes expressing GFP-moe. (G) Stage 14 oocyte, prior to in vitro

activation (pre). GFP-moe also decorates the overlying follicle cells. Oo: oocyte; da: dorsal appendage. (H) The same oocyte, post-activation in vitro. The arrowhead and arrow indicate corresponding regions of the cortex pre- and post-activation.(Ga–Hb) Higher power images of the cortical actin cytoskeleton pre- (Ga, Gb) and post- (Ha, Hb) activation in the regions corresponding to the arrowheads and arrows in (G) and (H). (I) Confocal section of a newly fertilized embryo expressing GFP-moe.

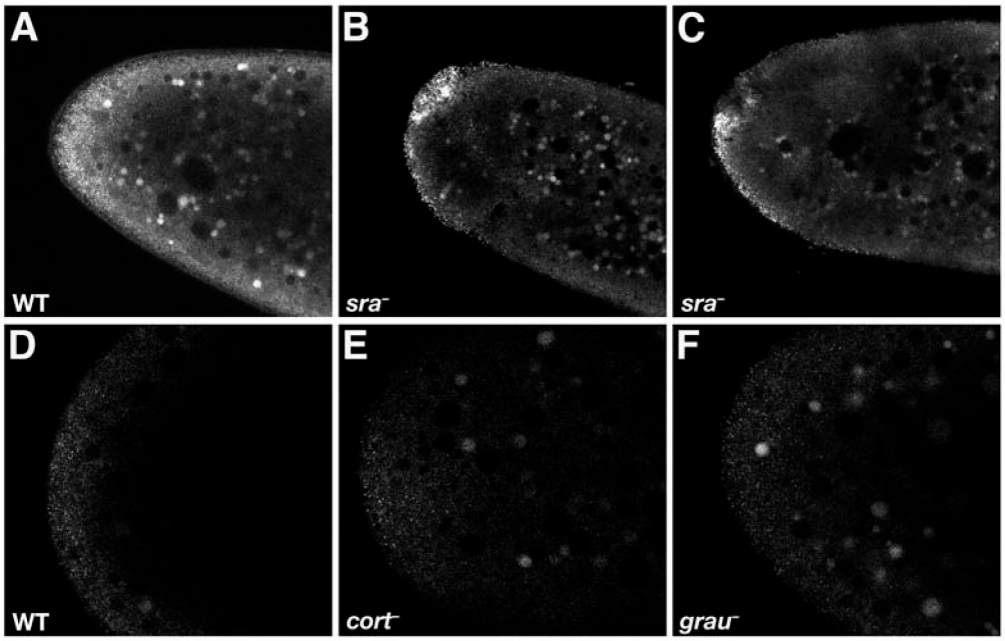

Figure 5. Effect of mutations that disrupt egg activation on *bcd* localization in the early embryo

Single confocal sections of the anterior of early embryos expressing *bcd*GFP* in (A,D) wild type, (B,C) sra^{A108}/sra^{687}, (E) $cort^{QW55}/cort^{RH65}$, and (F) grau mutant embryos. *bcd* mRNA remains associated with the anterior cortex in large foci in *sra* mutant embryos but is disperse in *cort* and *grau* mutant embryos.

Table 1

Temporal analysis of RNA particle dynamics

Stage	Static	Jiggling	Directed	Total
		bicoid RNA		
10b-12	25 (11%)	151 (66%)	52 (23%)	228
13	22 (21%)	63 (63%)	17 (16%)	104
14	39 (51%)	29 (38%)	8 (11%)	78
		nanos RNA		
10b-12	73 (86%)	12 (14%)	0	85
13	83 (93%)	6 (7%)	0	89
14	40 (91%)	4 (9%)	0	44